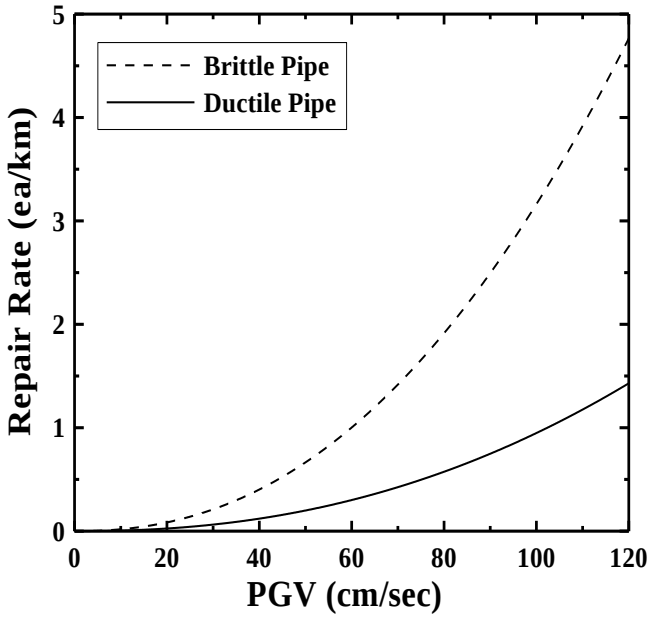

Fig. 1. Fragility curve of buried pipelines provided by HAZUS with the repair rate (RR) given as a function of the peak ground velocity (PGV) (FEMA, 1999)

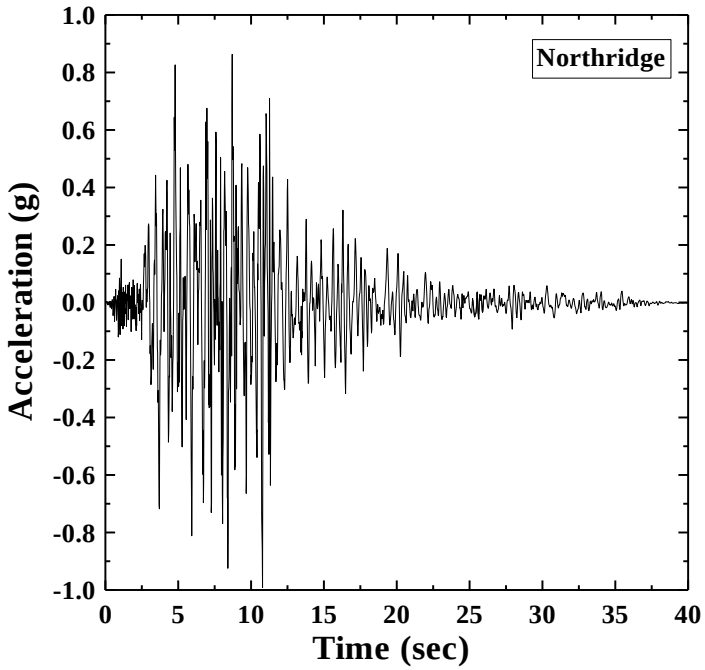

Fig. 2. History of ground acceleration record during the 17 January 1994 Northridge (M_w = 6.7) earthquake (COSMOS, 2010)

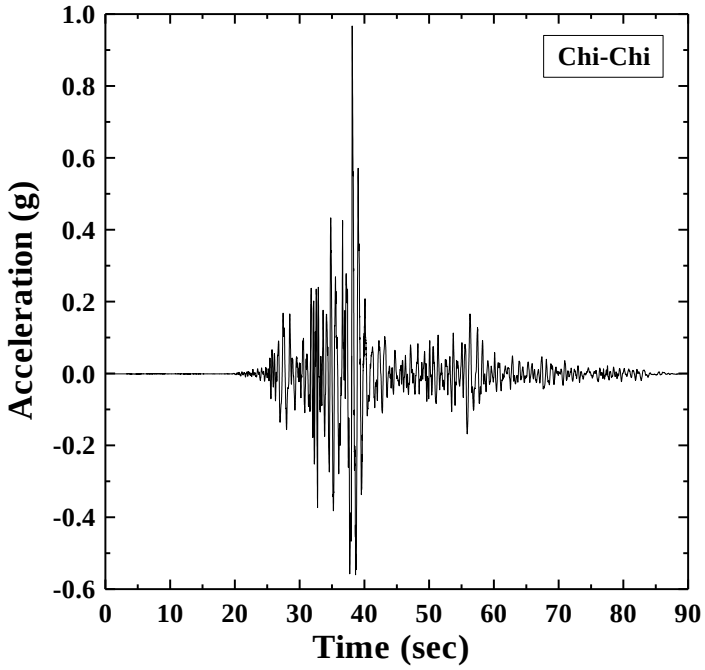

Fig. 3. History of ground acceleration record during the 21 September 1999 Chi-Chi (M_w = 7.6) earthquake (COSMOS, 2010)

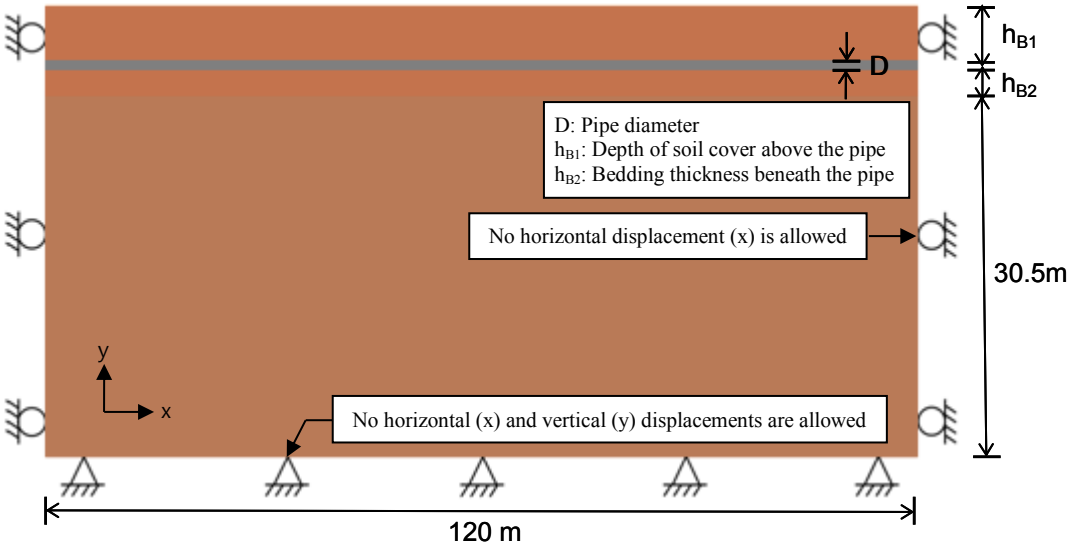

Fig. 4. Configuration of numerical model associated with pipeline and an in-situ soil depth and width of 30.5 m and 120 m, respectively

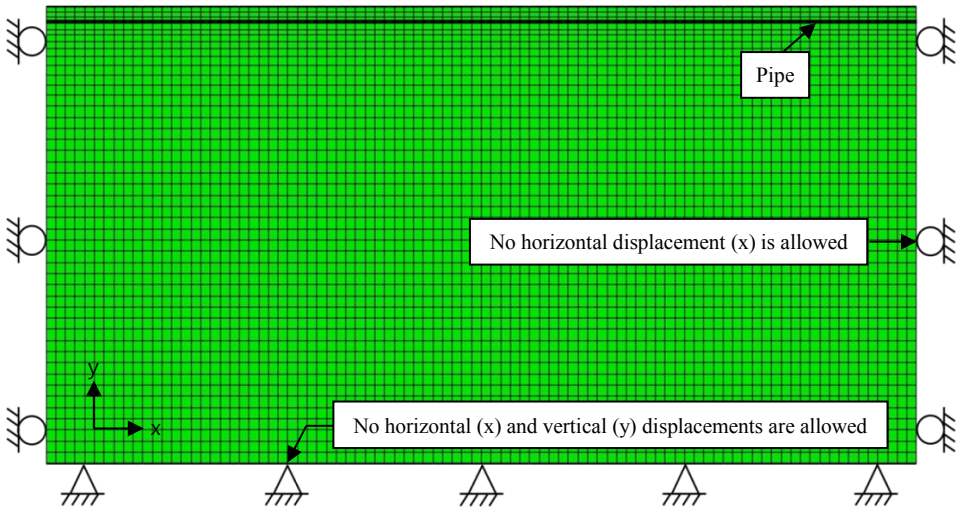

Fig. 5. Finite element mesh configuration and boundary conditions for pipelines and an in-situ soil depth and width of 30.5 m and 120 m, respectively

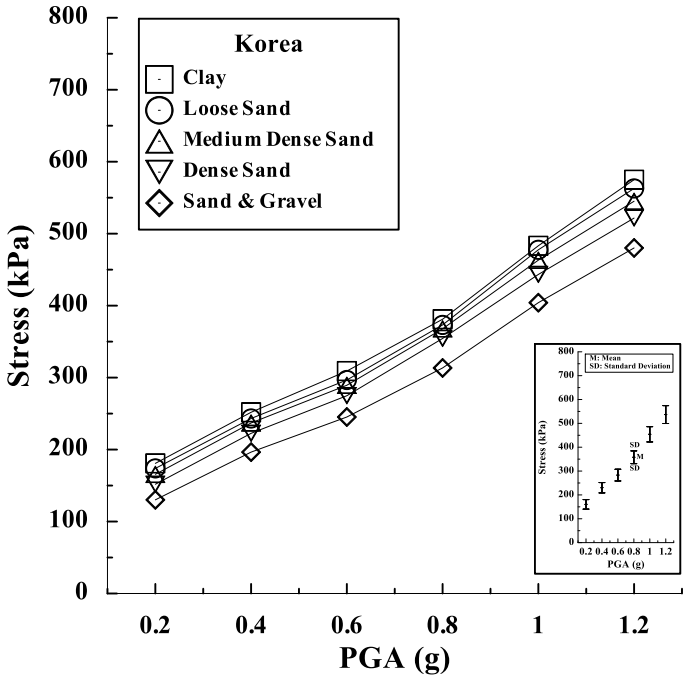

(a) Korea

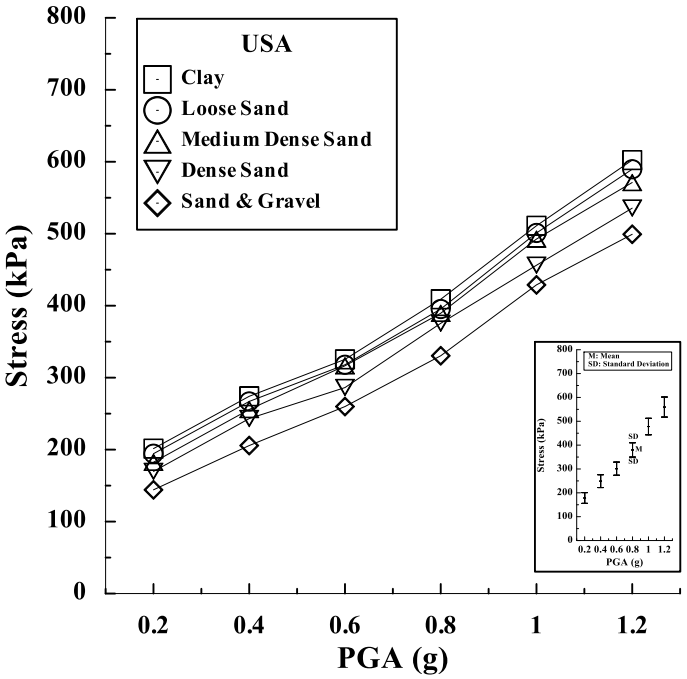

(b) The US

Fig. 6. Stress of ductile pipeline mobilized by earthquake loadings with respect to peak ground acceleration (PGA) in various in-situ ground conditions. Values are derived from finite element analysis (see Fig. 5 and Sect. 4.2.1 for further details)

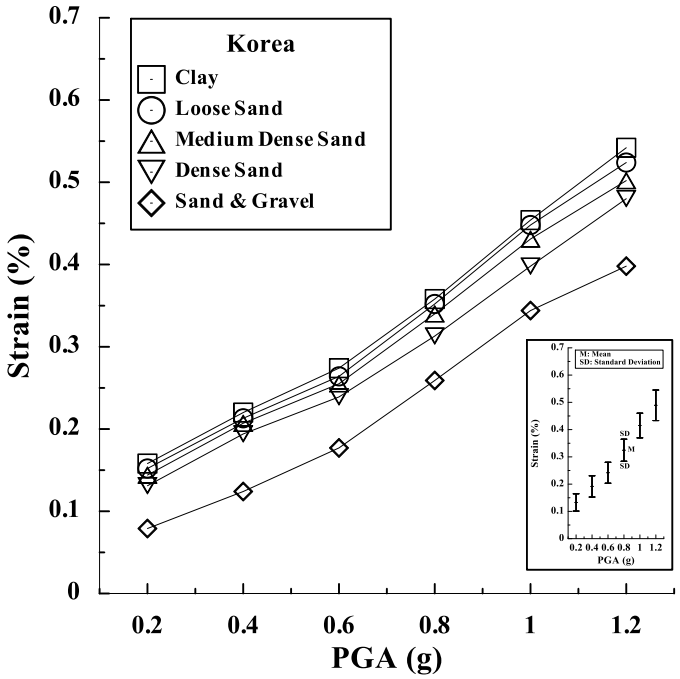

(a) Korea

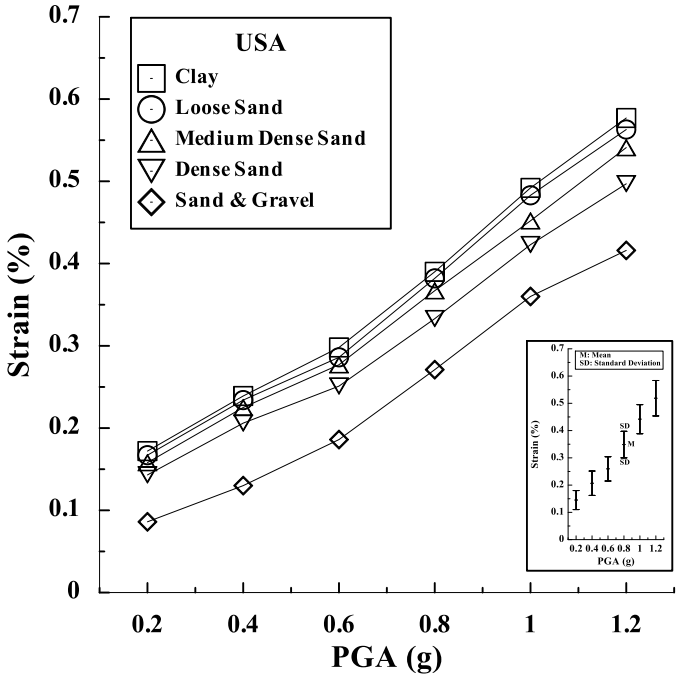

(b) The US

Fig. 7. Strain (%) of ductile pipeline mobilized by earthquake loadings with respect to peak ground acceleration (PGA) in various in-situ ground conditions. Values are derived from finite element analysis (see Fig. 5 and Sect. 4.2.1 for further details)

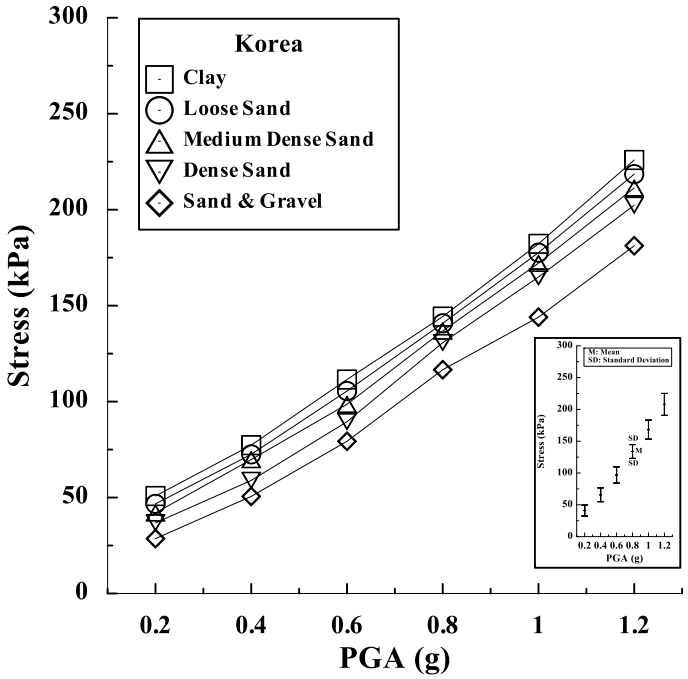

(a) Korea

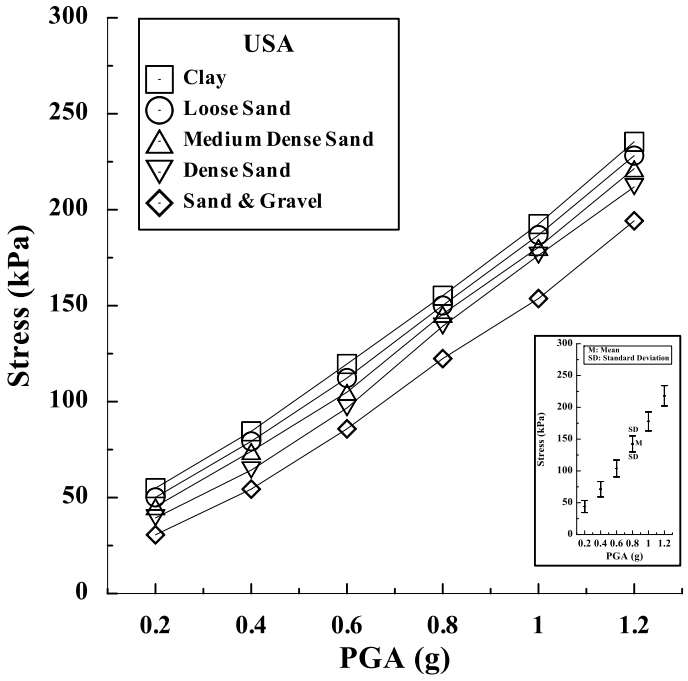

(b) The US

Fig. 8. Stress of brittle pipeline mobilized by earthquake loadings with respect to peak ground acceleration (PGA) in various in-situ ground conditions. Values are derived from finite element analysis (see Fig. 5 and Sect. 4.2.2 for further details)

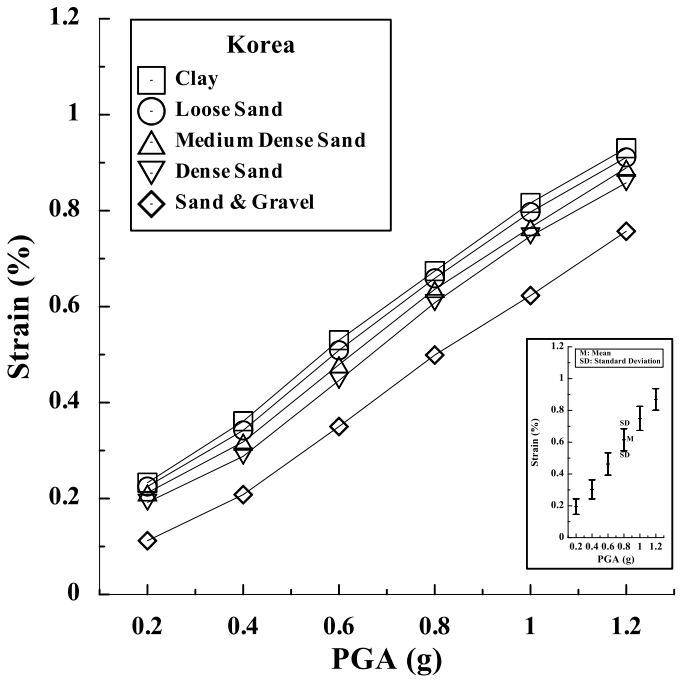

(a) Korea

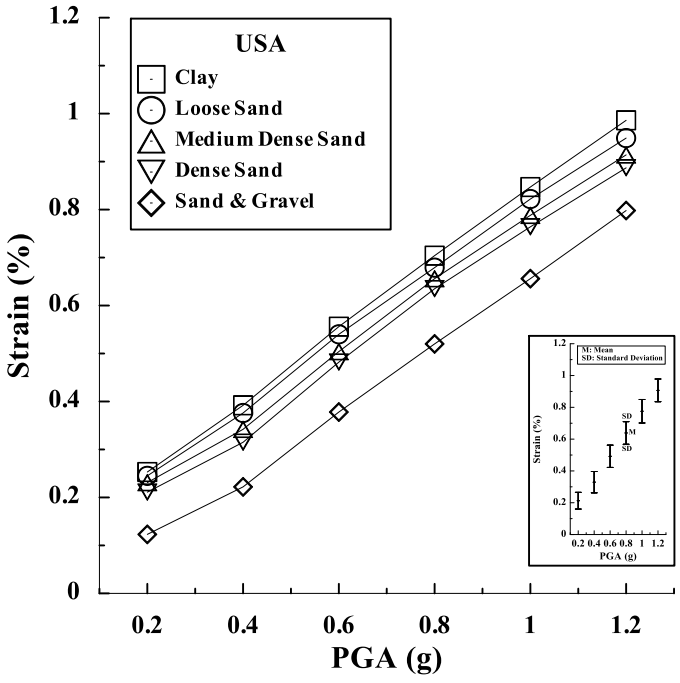

(b) The US

Fig. 9. Strain (%) of brittle pipeline mobilized by earthquake loadings with respect to peak ground acceleration (PGA) in various in-situ ground conditions. Values are derived from finite element analysis (see Fig. 5 and Sect. 4.2.2 for further details)